

European Association for the  
Development of Renewable Energies,  
Environment and Power Quality



International Conference on Renewable Energies and Power  
Quality (ICREPQ'09)

Valencia (Spain), 15th to 17th April, 2009

## Analysis and NN-Based Control of Doubly Fed Induction Generator in Wind Power Generation

Orlando Manuel Soares<sup>1</sup>, Henrique Nuno Gonçalves<sup>2</sup>, António Pina Martins<sup>2</sup> and Adriano Silva Carvalho<sup>2</sup>

<sup>1</sup> Escola Superior de Tecnologia e de Gestão

Instituto Politécnico de Bragança

Campus de Santa Apolónia, 5301-857 Bragança, Portugal

E-mail: osoares@ipb.pt

<sup>2</sup> Faculdade de Engenharia da Universidade do Porto

Rua Dr. Roberto Frias, 4200-465 Porto, Portugal

E-mail: henrique@fe.up.pt, ajm@fe.up.pt and asc@fe.up.pt

**Abstract.** With the increasing size of wind power generation it is required to perform power system stability analysis that uses dynamic wind generator models.

In this paper are presented all the wind power system components, including the turbine, the generator, the power electronic converter and controllers. The aim is to study the Doubly Fed Induction Generator (DFIG) operation and its connection to the power system, either during normal operation or during transient grid fault events.

Two different control system design technologies are present, the first is performed by standard PI controllers and the second is based on artificial neural networks.

### Keywords

Wind power generation, Simulation, Control, Neural networks, Doubly fed induction generator.

### 1. Introduction

The impact of wind farms on the power systems has mainly been on the voltage of the local feeder and the local substation. As the size of the wind farms increases on as well as the level of penetration into power system, the impact on the power system is not only local but has influence on a much larger part of the system including the unit commitment and dispatch.

Present growth and related installed power level make necessary to develop wind farm control capabilities and strategies that had features equivalent to conventional power plants. These features include capabilities to control the output power of the total wind farm, control of the reactive power and robustness to faults in the grid. This will enable wind power plants to be included as active components of the power supply system, [1]-[2].

The purpose of the control system is to manage the safe, automatic operation of the turbine, within a framework of optimising generated power. This reduces operating

costs, provides consistent dynamic response and improved product quality, and helps to ensure safety by maximizing the capture of the wind energy due to minimization of turbine loads.

Many wind power turbines with related control strategies were developed by so many authors. These strategies include fixed and variable wind turbines with the same purpose of extracting the maximum wind power with the best quality service.

This paper describes wind generation models for operation within power system in order to perform stability analysis and turbine control to maximize the power generated with the lowest impact on the grid voltage and frequency during normal operation and under several disturbances, such as a transmission line earth fault. The discussed methods considers wind turbines based on induction generator and a grid-connected converter with constant or variable blade angle applied to variable speed wind turbines. The study is performed within the multiple technologies design tool Matlab/Simulink, [3].

Two power control techniques were used: PI controllers and artificial neural networks. The dynamic control joins different strategies that will ensure better stability and power regulation generated by the wind turbine. Those strategies with intelligent control techniques, such as artificial neural networks, allow the increase of robustness, performance, capacity and flexibility.

### 2. The Control Structure Model

The overall structure of the model that is being used in this work includes aerodynamic, mechanical and electric system components, with an overall control system model. The electric model interfaces with the grid model, whereas the aerodynamic model interfaces to the wind model, [1]-[2].

### A. Turbine and Drive-Train Subsystem

The aerodynamic model is appropriate to a wind power generating system turbine that tracks a prescribed torque-speed profile, function of the power to be delivered. Variable speed operation is introduced to gain efficiency in generating power. The torque-velocity wind turbine characteristic allows the establishment of several possible wind turbine operation control strategies. This means that  $C_p$  can be calculated as by control of the aerodynamic model and used to determine the aerodynamic power  $P_{ae}$ , [1]-[2].

$$P_{ae} = \frac{1}{2} \rho \pi R^2 v^3 C_p(\lambda, \beta) \quad (1)$$

The mechanical model was selected with emphasis to include only parts of the dynamic structure, that are important to the interaction with grid, i.e. which influence significantly on the fluctuations of the power. Thus, only the drive train is considered in the first place because this part of the wind turbine has the most significant influence on the power fluctuations. The state space equations can be obtained from the mechanical model to perform the drive train simulation, [1]-[2].

### B. Doubly Fed Induction Generator

The induction generator model adopted in this work is the qd0 stationary rotating reference frame model because it is more appropriate to simulate induction machine transients. The mathematical transformation abc to qd0 facilitates the computation of the transient solution of the induction generator model by transforming the differential equations with time-varying inductances, [4]-[7].

$$\begin{cases} v_{qs} = r_s i_{qs} + \omega \lambda_{ds} + \frac{d\lambda_{qs}}{dt} \\ v_{ds} = r_s i_{ds} - \omega \lambda_{qs} + \frac{d\lambda_{ds}}{dt} \end{cases} \quad (2)$$

$$\begin{cases} v'_{qr} = r'_r i'_{qr} + (\omega - \omega_r) \lambda'_{dr} + \frac{d\lambda'_{qr}}{dt} \\ v'_{dr} = r'_r i'_{dr} - (\omega - \omega_r) \lambda'_{qr} + \frac{d\lambda'_{dr}}{dt} \end{cases} \quad (3)$$

$$T_{em} \approx \frac{3}{2} \frac{P}{2} L_m (i'_{dr} i_{qs} - i'_{qr} i_{ds}) \quad (4)$$

The study of the induction generator reveals the stability and performance in transient condition of the induction generator to mechanical input torque when connecting the doubly fed induction generator to the power system.

### C. Power Electronics Converters

Using a PWM back-to-back converter the voltage fluctuations, frequency, and output power from the wind turbine can be controlled. The converter takes control on the fluctuating non-grid frequency output power of the induction generator to a DC voltage level that will be injected through a PWM-converter into a three-phase grid frequency power, [8]-[9].

The electronic power converter used was a back-to-back converter witch allows to inject and get current from the rotor with current flow in both sides, [4], [6].

## 3. The PI Control Structure Model

It is intended to control the power delivered by each generator in a way to optimize the operation of the wind park with propose to deliver the maximum active power to the grid in conditions of quality of service and safety. Also it intends to control the reactive power flow according to specified needs and dispatch. Thus, an adequate control strategy cans, [9]:

- 1) Control the active power supplied by the turbine in order to optimize the operating point;
- 2) Limit the active power in the case of high wind speed;
- 3) Control the interchange of the reactive power between the generator and the grid, especially in the case of weak grids, where voltage fluctuations can occur;
- 4) Guarantee the quality of service of the wind park, namely the grid voltage;
- 5) Minimize the exploration and maintenance costs of the wind park.

A typical configuration is illustrated in Figure 1 and it is based on a DFIG.

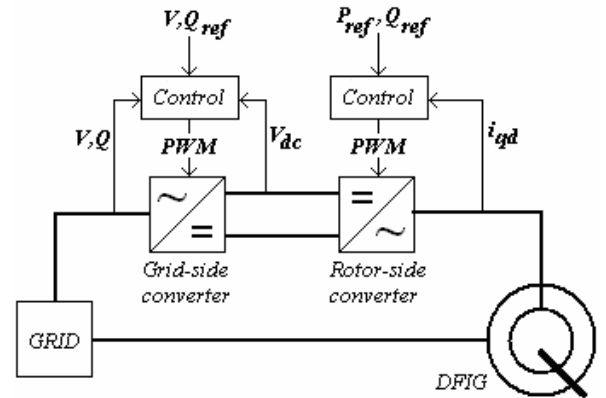


Fig. 1. General DFIG control structure.

The aim of the rotor- side converter is the independent control of the active power and reactive power witch are controlled, not directly, but by the control of the rotor current. The aim of the grid-side converter is to keep constant the DC voltage in the intermediate capacitor in order to guarantee an operation of the converter with power factor equal to one guaranteeing only the exchange of reactive power through the stator, [9].

In Figure 1,  $P_{ref}$  is the optimal value for the active power and is gotten from the characteristic of the turbine for the speed of rotation of the rotor and the pitch angle. The value of  $Q_{ref}$  is defined in a way to keep the voltage stable at the grid connection point.

Several strategies of control have been vastly argued in literature. The use of vector control allows the decoupling of rotor current components q and d in order to control the flow of the active and reactive energies, [4], [9].

### A. Grid-Side Converter Control

The main objective of the grid-side converter is to keep a constant DC link voltage independent of the value and direction of the rotor power flow. For this, a vector control strategy is used considering a referential oriented with the position of the voltages of the stator or grid. This allows independent control of the active and the reactive power between the converter and the grid.

For the internal control loop it is necessary to design the PI controllers' functions, which are obtained by application of the Laplace transform of (5) that represents the grid-side converter voltages in its dq components, [9].

$$\begin{cases} v_q = Ri_q + L \frac{di_q}{dt} + \omega_e Li_d + v_{q1} \\ v_d = Ri_d + L \frac{di_d}{dt} - \omega_e Li_q + v_{d1} \end{cases} \quad (5)$$

Using the Laplace transformation

$$\begin{cases} v_q = (R + sL)i_q + \omega_e Li_d + v_{q1} \\ v_d = (R + sL)i_d - \omega_e Li_q + v_{d1} \end{cases} \quad (6)$$

Assigning in the previous equations:

$$\begin{cases} v'_q = (R + sL)i_q \\ v'_d = (R + sL)i_d \end{cases} \quad (7)$$

the following equations can be used to design the current control loops, [9]:

$$F(s) = \frac{i_q}{v'_q} = \frac{i_d}{v'_d} = \frac{1}{R + sL} \quad (8)$$

Replacing (7) in (6), respectively, and being  $v_q(s) = 0$ , the reference for the voltages values  $v_{q\_ref}$  and  $v_{d\_ref}$  can be obtained by:

$$\begin{cases} v_{q\_ref} = -v'_q - \omega_e Li_d + v_q \\ v_{d\_ref} = -v'_d + \omega_e Li_q + v_d \end{cases} \quad (9)$$

These reference values are the inputs used in the PWM converter in order to guarantee the DC voltage level and required power factor.

The grid-side converter control diagram is shown in Figure 2, for which normalized design techniques can be applied.

### B. Rotor-Side Converter Control

The control of the induction generator rotor is carried through in a synchronous rotating dq referential, with the d-axis aligned with the stator flux position. In this way decoupling between the electromagnetic torque and rotor the magnetizing current can be obtained. The PWM converter acts on the generator rotor and the control is done by means of the signals of the rotor and the stator currents, the stator voltage and the rotor position.

Figure 3 presents the controller of the rotor-side converter control diagram. The control design of the

rotor-side converter can be made in a similar way as the one considered for the grid-side converter. The rotor voltage in the dq referential can be obtained from (10).

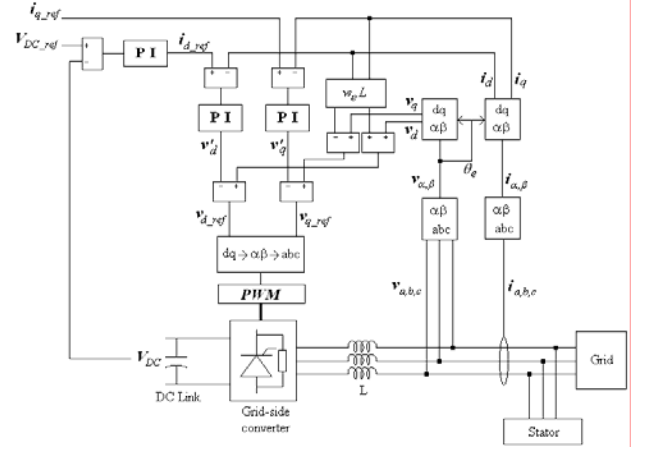


Fig. 2. Grid-side converter controller diagram.

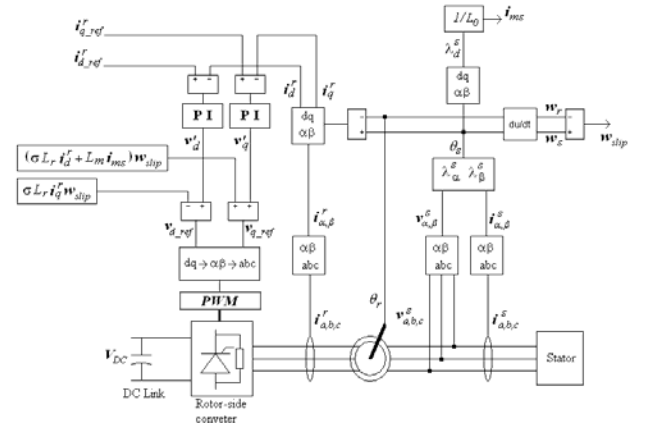


Fig. 3. Rotor-side converter controller diagram.

$$\begin{cases} v_d^r = R_r i_d^r + \sigma L_r \frac{di_d^r}{dt} \\ v_q^r = R_r i_q^r + \sigma L_r \frac{di_q^r}{dt} \end{cases} \quad (10)$$

The error signals  $i_d^r$  and  $i_q^r$  are applied to the PI controller to obtain the voltages  $v_d^r$  and  $v_q^r$ , respectively. To compensate the control are added the decoupling terms to the previous equations in order to get the reference voltages  $v_{d\_ref}^r$  and  $v_{q\_ref}^r$ , [9], in accordance with:

$$\begin{cases} v_{d\_ref}^r = v_d^r - \sigma L_r i_q^r \omega_{slip} \\ v_{q\_ref}^r = v_q^r + (L_m i_{ms} + \sigma L_r i_d^r) \omega_{slip} \end{cases} \quad (11)$$

## 4. The NN Controller Structure Model

The new control system will use a NN to substitute some blocks of the traditional system of vector control, [10]-[12].

Thus, it is intended to present a control system based on

neural networks to be used in the control system alternatively to the one based on PI controllers, with the intention of efficiently extract the wind energy, i.e. to be able to extract the maximum power of the turbine during some situations of functioning through the estimation of the control parameters for the grid-side and rotor-side converters.

#### A. NN Controllers Architecture

The learning algorithm updates the values of the weights and bias values according to the descendent gradient with momentum factor and adaptive learning ratio, also indicated in Table I, as well as the activation functions used in each layer and respective parameter, [13].

The sampling frequency is 20 kHz. The numbers of time delays used in each layer of the neural network had been adjusted as resulted of several simulations.

The used learning input-output pairs were generated by several system simulations and contemplate operation points with the machine operating in a zone below the synchronism speed, where active power is supplied to the rotor of the machine; in a zone near the synchronism speed, where the active power flow in the rotor of the machine is practically null; and a zone above the synchronism speed, where the machine supplies active power to the grid through the stator and the rotor.

TABLE I. - NN layers parameters.

	1st Hidden Layer	2nd Hidden Layer	Output Layer
Activation function - $\phi$	Symmetric sigmoidal	Symmetric sigmoidal	Linear
Parameter - $\gamma$	2,0	2,0	-
Parameter - $a$	2,0	2,0	-
Parameter - $c$	-1,0	-1,0	-
Learning coefficient - $\eta$	0,05		
Momentum - $\alpha$	0,9		

For the rotor-side controller was used a 7-15-10-2 neural network configuration as is shown in Table II, where the inputs are the stator and rotor currents, the rotor-side reference currents and the rotor angular speed, and the outputs are the reference voltages to control the rotor-side converter.

For the grid-side controller was used a 7-18-8-2 neural network configuration as is shown in Table III, where the inputs are the stator voltages and currents, the grid-side reference currents, and the angular frequency  $\omega_s$ , and the outputs are the reference voltages to control the rotor-side converter.

TABLE II. - NN architecture and training parameters of the rotor-side controller.

	1st Hidden Layer	2nd Hidden Layer	Output Layer
No of inputs	7 inputs		
No of neurons	15	10	2
No input-output training pair	80.000		
No of iterations	1633		
Error	< 9,98E-6		

TABLE III. - NN architecture and training parameters of the grid-side controller.

	1st Hidden Layer	2nd Hidden Layer	Output Layer
No of inputs	7 inputs		
No of neurons	18	8	2
No input-output training pair	80.000		
No of iterations	1313		
Error	< 9,99E-6		

## 4. Results

#### A. Reactive Power Control

In this simulation it is intended to vary the reference value of the reactive power in two steps, a first positive of 0.2 p.u., and the other equal to -0,4 p.u. Figures 4 and 5 show the signals of the reference voltages generated by the current regulators for the controllers of the grid-side and the rotor-side converters with NN (in the blue colour) and PIs (in the green colour).

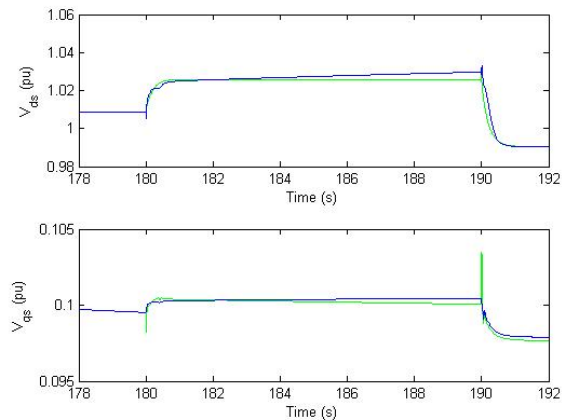


Fig. 4. Reference grid-side voltage  $v_{dq}$ , due to reactive power control.

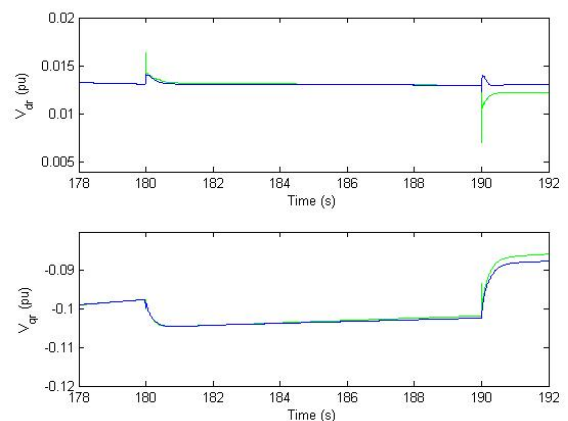


Fig. 5. Reference rotor-side voltage  $v_{dq}$ , due to reactive power control.

It can be verified that the behaviour of the system with the NN is identical to the system with PI controllers. The response of the NN, face to the PI controllers' response presents, generally, lesser transient amplitudes and faster response.

As expected, the quadrature component of the reference voltage has a significant level to the control of the reactive power. The following figure represents the active power and reactive power delivered to the grid.

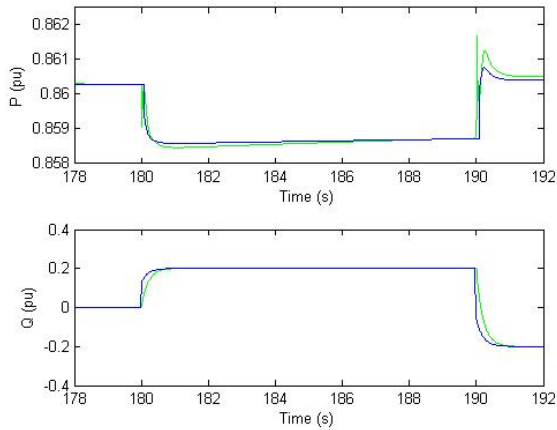


Fig. 6. Active power and reactive power, due to reactive power control.

It can be verified that the NN response is more desirable; it has a faster response to reach the stationary regimen, namely the value of the active power after 190 seconds.

### B. Active Power Control

In a second simulation it is intended to verify the system response due to a variation of the active power flow, obtained through a variation in the quadrature component of the rotor current. This variation consisted in applying a negative pulse of amplitude equal to 0,2 p.u. The reference voltage signals for the controllers of the grid-side and rotor-side converters have been registered in Figures 7 and 8, and the power flows in Figure 9.

Also in this situation, the maximum difference verified between the two control types is less than 0.5%, as in the previous case. The NNs present, generally, transients of lesser amplitude and greater speed to reach the steady-state condition. This behaviour is also verified in the main electric and mechanical variables.

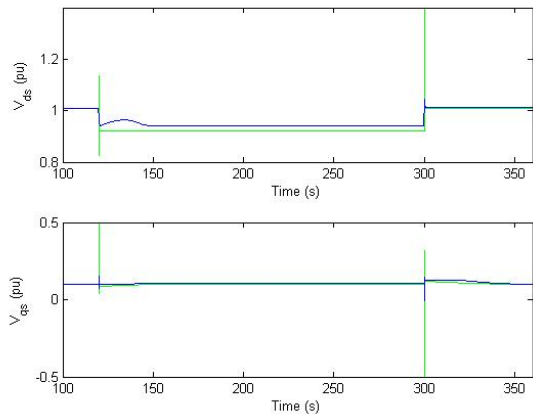


Fig. 7. Reference grid-side voltage  $v_{dq}$ , due active power control.

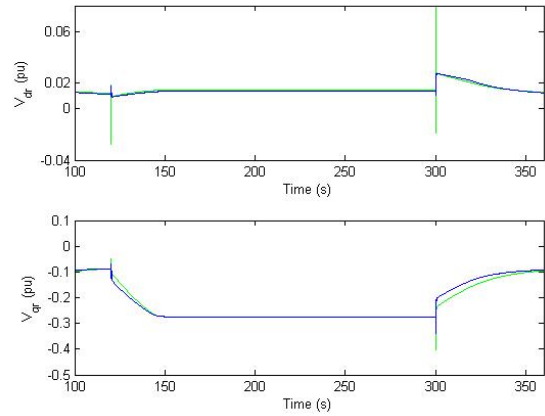


Fig. 8. Reference rotor-side voltage  $v_{dq}$ , due to active power control.

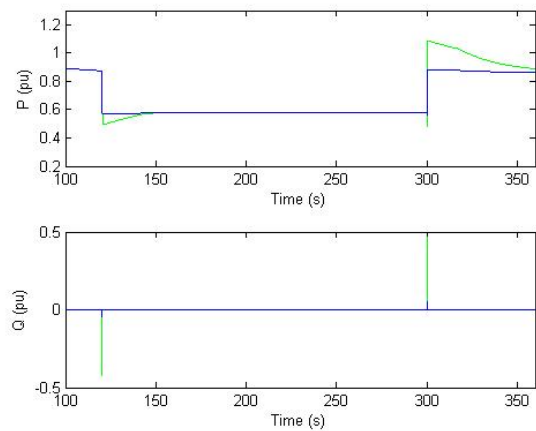


Fig. 9. Active power and reactive power, due to active power control.

### C. Phase-to-Earth Fault

A phase-to-earth fault in a line of the electrical network located near the wind park occurred at  $t=180$  s with a duration of 180 ms. The fault impedance was 1 m $\Omega$ . Figures 10 and 11 show again the signals of the reference voltages used to control the stator-side and rotor-side converters, respectively, with NNs (in the blue colour) and PIs (in the green colour).

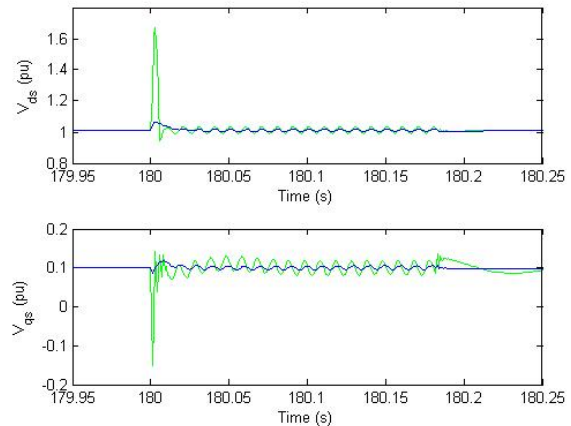


Fig. 10. Reference grid-side voltage  $v_{dq}$ , due to a phase-to-earth fault.

During the fault period, it was verified that the NNs response presents better results than the system using PI controllers; beside the peaks already related previously in the transitions, they present a lesser ripple. It is important to relate that in the direct component of the stator voltage with PI controllers the peaks can reach about 1,7 p.u. and that can cause some unwanted effects in the electronic devices used in the converters.

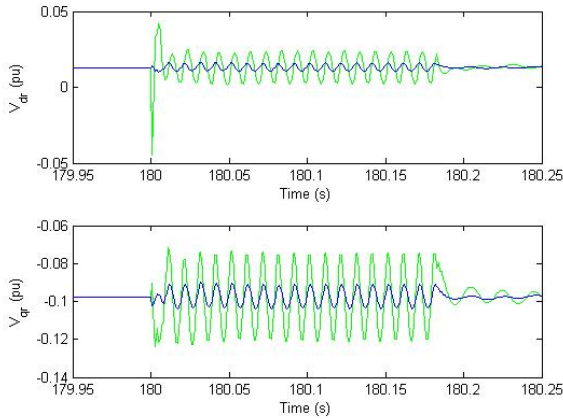


Fig. 11. Reference rotor-side voltage  $v_{dq}$ , due to a phase-to-earth fault.

In Figure 12 it can be verified that the disturbances caused in the active power and reactive power delivered to the grid are smoother with the use of the NNs.

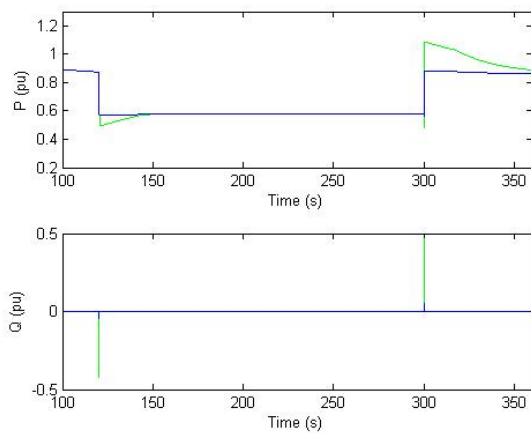


Fig. 12. Active power and reactive power, due to a phase-to-earth fault.

#### 4. Conclusion

The NN-based system that estimates the control parameters of the generator shown satisfactory characteristics, as was verified in the presented results.

Some differences in the controllers responses using neural networks can be noticed, namely three positive and advantageous aspects: transient regimes present smaller overshoots, or absence of them in some cases, what corresponds to less severe transitions; a faster response, i.e. the system retakes the permanent regimen in lesser time; and smaller oscillatory behaviour.

It was demonstrated that the reference signals for the grid-side and rotor-side converters of the DFIG can be obtained using control systems based in NNs. These can substitute most of the blocks of a conventional control system, and with the referred advantages.

#### References

- [1] J. F. Walker, N. Jenkins, "Wind Energy Technology", John Wiley & Sons, Ltd, 1997.
- [2] T. Ackermann, "Wind Power in Power Systems", John Wiley & Sons, Ltd, England, 2005.
- [3] C. Ong, "Dynamic Simulation of Electric Machinery", Prentice Hall, 1998.
- [4] A. Tapia, G. Tapia, J. X. Ostolaza, J. R. Saenz, R. Criado, J. L. Berasategui, "Reactive power control of a wind farm made up with doubly fed induction generators", (I) and (II), *IEEE Porto Power Tech Conference*, 2001.
- [5] J. G. Sloomweg, H. Polinder, W. L. Kling, "Initialization of wind turbine models in power system dynamics simulations", *IEEE Porto Power Tech Conference*, 2001.
- [6] A. Tapia, G. Tapia, X. Ostolaza, E. Fernández, J. R. Saenz, "Modeling and dynamic regulation of a wind farm", *VII IEEE International Power Electronics Congress, CIEP 2000*, pp. 293-297, Acapulco, Mexico, 2000.
- [7] J. L. Rodríguez-Amenedo, S. Arnalte, J. C. Burgos, "Automatic generation control of a wind farm with variable speed wind turbines", *IEEE Transactions on Energy Conversion*, vol. 17, no 2, pp. 279-284, 2002.
- [8] J. G. Sloomweg, H. Polinder, W.L. Kling, "Dynamic modeling of a wind turbine with direct drive synchronous generator and back to back voltage source converter and its controls", *European Wind Energy Conference and Exhibition*, Copenhagen, Denmark, July, 2001.
- [9] R. Pena, J. C. Clare, G. M. Asher, "Doubly fed induction generator using back-to-back PWM converters and its application to variable-speed wind-energy generation", *IEE Proc.-Elect. Power Appl.*, vol. 143, no 3, May 1996.
- [10] S. Haykin, "Neural Networks. A Comprehensive Foundation", 2nd Edition, Prentice Hall, 1999.
- [11] M. G. Simões, B. K. Bose, "Neural network based estimation of feedback signals for vector controlled induction motor drives", *IEEE Transactions on Industry Applications*, vol. 31, no 3, pp. 620-629, May-June 1995.
- [12] F. M. de Azevedo, L. M. Brasil, R. C. L. de Oliveira, "Redes Neurais, com Aplicações em Controle e em Sistemas Especialistas", Florianópolis: Bookstore, 2000.
- [13] H. Demuth, M. Beale, "Neural Network Toolbox for use with MATLAB", User's Guide, MathWorks, Inc., 1992.